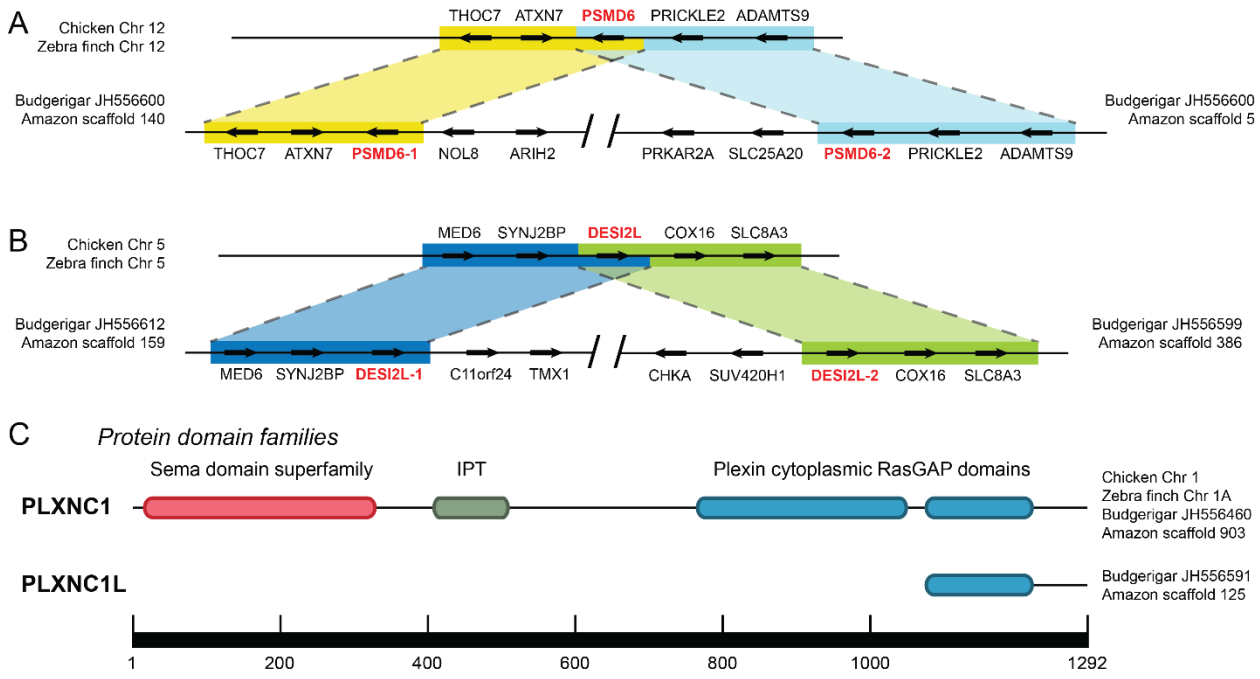

Figure S1. Novel gene duplications in parrots. Related to Table 1. (A-B) Depiction of chromosomal rearrangements unique to parrots and likely implicated in the generation of parrot-specific duplications of (A) PSMD6, a 26S proteasome subunit that colocalizes with DNA damage foci in cells that have suffered genotoxic damage, helping to ensure that these cells are targeted for senescence [S1], and (B) DESI2L, an apoptosis regulator and part of the early response to DNA damage [S2]. Further highlighting DNA repair and control of cell proliferation as important pathways in the evolution of parrots, several additional duplicated genes in parrots also regulate genomic stability and cell senescence: SUN2, which together with the known longevity factor SUN1 is part of the inner nuclear envelope and interacts with a DNA-dependent protein kinase (DNAPK) complex that functions in DNA nonhomologous end joining repair in response to DNA damage [S3]; SIDT1, implicated in intercellular transfer of siRNAs and the spread of chemoresistance in cancer [S4]; and MXRA7, member of a gene family involved in cell adhesion, matrix remodeling, cancer spread, and metastasis [S5]. (C) Alignment of conserved avian PLXNC1 and its parrot lineage-specific duplicate, PLXNC1L, depicting predicted protein domains. Numbers in scale indicate amino acid residue position in A. aestiva PLXNC1 ortholog. IPT, Immunoglobulin-like fold Plexin Transcription factors. See Table 1 for a summary and Data S1F-I for a complete list of novel genes duplicated and expanded in parrots.

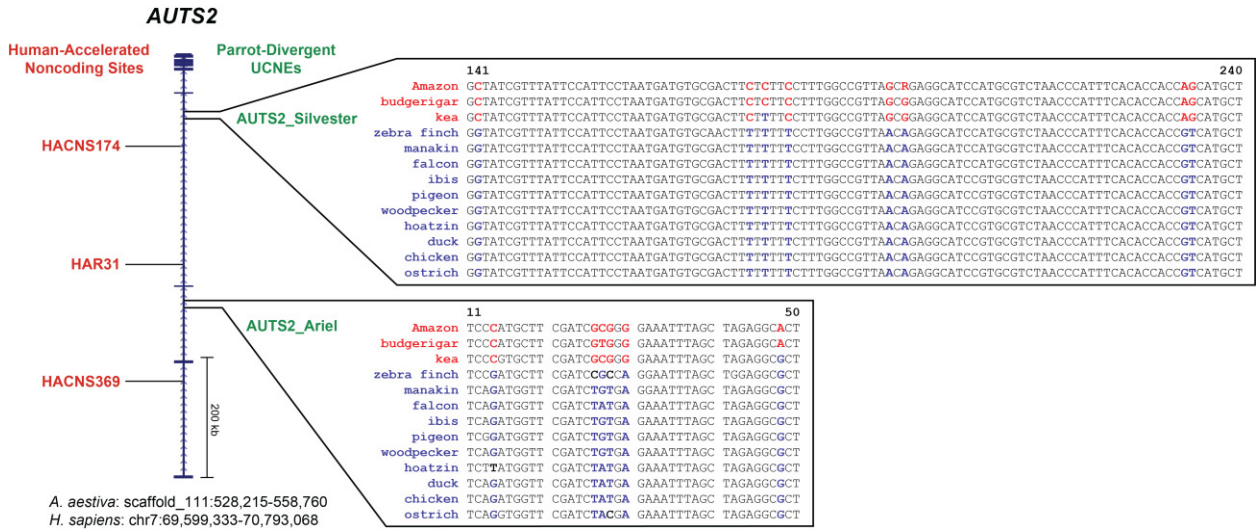

Figure S2. Parrot-specific divergence in ultra-conserved noncoding elements (UCNEs). Related to Table 2. Associated with AUTS2. Noncoding regions with evidence of accelerated evolution in the human lineage are indicated in red text at left (haCNS, human accelerated conserved noncoding sequences [S6]; HAR, human accelerated regions [S7]), and UCNEs with evidence of lineage-specific selection in parrots are indicated in green at right, with regions containing parrot-specific polymorphisms shown in the expansions at the far right. Multi-species sequence alignments of these regions reveal substitutions unique to parrots (in red) and non-parrot consensus polymorphisms (in blue). Numbers indicate nucleotide position within UCNEs. Further details and full list of UCNEs and associated genes divergent in parrots are described in STAR Methods: UCNEs.

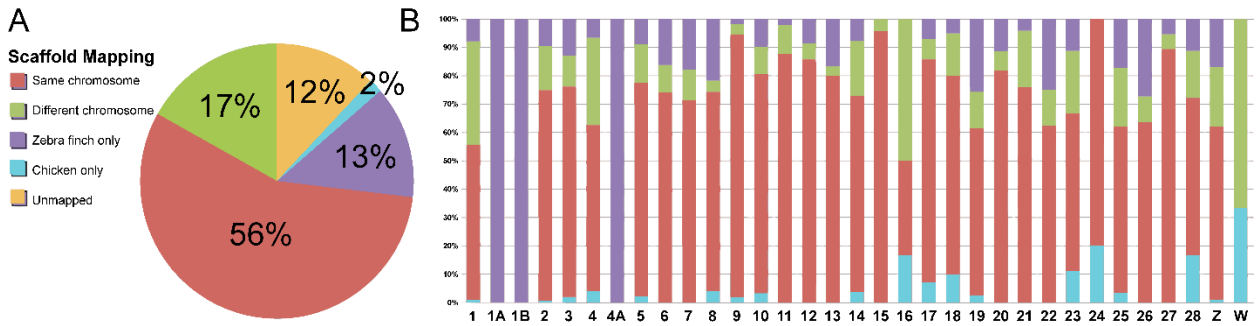

Figure S3. Comparative genomic analysis of Blue-fronted amazon and avian model species. Related to STAR Methods. Graphical depiction of *Amazona aestiva* scaffolds mapped onto the chicken and zebra finch genomes: A) scaffold mapping categories and corresponding percentages; B) chromosomal distribution of scaffold mapping categories.

Blue-fronted Amazon scaffolds were mapped to the genomes of chicken and zebra finch using blastn. Over half (56%) of the scaffolds mapped to the same chromosomes in both non-parrot species, indicating good conservation at the chromosome level (A, in red). Another considerable fraction of the scaffolds (17%) mapped to different chromosomes in the two non-parrot species (A, in green), likely reflecting inter-chromosomal rearrangements. The Blue-fronted Amazon genome shared more unique regions with zebra finch (13%) than with chicken (2%) (A, in purple and blue, respectively), consistent with their phylogenetic relationships [S8]. For the most part, individual chromosomes (depicted in B) showed comparable proportions of these different mapping categories. The few exceptions consisted of scaffolds mapping onto chromosomes that are lacking as a separate chromosomal unit in chicken (i.e. zebra finch chromosomes 1A, 1B, and 4A) or unsequenced in zebra finch (i.e. chromosome W).

We found that 12% of Blue-fronted Amazon scaffolds did not map to either chicken or zebra finch genomes (A, in orange). This corresponds to 1.1 Mb, 0.09% of the total genome sequence length. To rule out contamination by bacterial DNA a BLAST search was performed for highly similar sequences between these scaffolds and the entirety of the bacterial nucleotide database available at GenBank using an e-value cutoff of 1e-10. None of the scaffolds had any significant alignment with bacterial sequences. Using the same approach, scaffolds that did not map to either genome were subsequently aligned to the genomes of the budgerigar, Kea, and Puerto Rican Parrot. All but 37 scaffolds (0.012% of the total genome sequence length) aligned to one or more of the other parrot genomes, suggesting that these 37 represent sequences specific to the Blue-fronted Amazon. Thus, the 12% of scaffold sequences uniquely found in parrots likely reflects true lineage-specific sequence divergence in this lineage.

Longevity group*	Species abbrev.	Species Name	Common Name	Adult weight (g)	Condition	Maximum Observed Longevity (years)	Maximum expected longevity**	Longevity Deviation (%)
RL	Bre	*Balearica regulorum*	Grey Crowned Crane	3372	Captivity	27.2	51.1	-46.8
RL	Can	*Calypte anna*	Anna's Hummingbird	4.4	Wild	8.5	8.2	3.7
RL	Cvo	*Charadrius vociferus*	Killdeer	88	Wild	10.9	14.1	-22.7
RL	Cst	*Colius striatus*	Speckled Mousebird	51	Captivity	11.5	17.9	-35.8
RL	Cca	*Cuculus canorus*	Common Cuckoo	111.5	Wild	12.9	14.7	-12.3
RL	Ppu	*Picoides pubescens*	Downy Woodpecker	25.6	Wild	11.9	11.3	5.3
RL	Ehe	*Eurypyga helias*	Sunbittern	210	Captivity	15	25.5	-41.2
RL	Gga	*Gallus gallus*	Red Junglefowl	779.8	Captivity	30	35.4	-15.3
RL	Hal	*Haliaeetus albicilla*	White-tailed Eagle	6696.5	Captivity	42	60.6	-30.7
RL	Hle	*Haliaeetus leucocephalus*	Bald Eagle	3175	Captivity	48	50.3	-4.6
RL	Mga	*Meleagris gallopavo*	Wild Turkey	6050	Wild	13	30.2	-57
RL	Nni	*Nipponia nippon*	Crested Ibis	1900	Captivity	25.8	44.2	-41.6
RL	Pcr	*Pelecanus crispus*	Dalmatian Pelican	9550	Captivity	35.3	66.2	-46.7
RL	Pca	*Phalacrocorax carbo*	Great Cormorant	3628.8	Wild	27.2	27.5	-1.1
RL	Pci	*Podiceps cristatus*	Great Crested Grebe	738.7	Wild	19.2	20.7	-7.3
RL	Sca	*Struthio camelus*	Ostrich	111000	Captivity	50	122.3	-59.1
HL	Aae	*Amazona aestiva*	Parrot	451	Captivity	49	30.9	58.6
HL	Cpe	*Chaetura pelagica*	Chimney Swift	22.8	Wild	15	11.1	35.1
HL	Cli	*Columba livia*	Rock Pigeon	358.7	Captivity	35	29.2	20
HL	Ega	*Egretta garzetta*	Little Egret	312	Wild	22.3	17.7	26
HL	Mun	*Melopsittacus undulatus*	Budgerigar	30	Captivity	21	15.7	33.8
HL	Nno	*Nestor notabilis*	Kea	867.5	Captivity	47	36.4	29.1
HL	Tal	*Tyto alba*	Common Barn Owl	580	Wild	34	19.8	71.7

Table S1. Lifespan data for wild and captive avian species. Related to Figure 1. List of avian species used in longevity analyses. *Longevity data were obtained from the AnAge database [S9], and are used as the basis for classification into regular-longevity (RL) or high-longevity (HL) groups. ** Estimated with $A(c)=5.07+-1.63xW^{0.23+-0.02}$ and $A(w)=4.75+-1.55xW^{0.17+-0.01}$, where A(c) is age in years for captivity birds, A(w) is age in years for wild birds, and W is weight in grams [S10].

Annotation Cluster 1: Enrichment Score: 4.12				
Annotation Category	**Annotation Term**	**Count**	***p* value**	**Benjamini**
UP_KEYWORDS	Kinetochore	11	3.50E-06	5.80E-04
UP_KEYWORDS	Mitosis	17	4.10E-06	4.60E-04
UP_KEYWORDS	Centromere	12	1.10E-05	7.10E-04
GOTERM_BP_DIRECT	sister chromatid cohesion	11	1.20E-05	1.80E-02
UP_KEYWORDS	Cell division	20	1.30E-05	7.10E-04
GOTERM_BP_DIRECT	cell division	19	4.00E-05	3.10E-02
GOTERM_BP_DIRECT	mitotic sister chromatid segregation	6	5.90E-05	3.10E-02
UP_KEYWORDS	Cell cycle	25	9.70E-05	3.60E-03
GOTERM_CC_DIRECT	condensed chromosome kinetochore	9	1.00E-04	1.80E-02
GOTERM_BP_DIRECT	mitotic nuclear division	15	1.10E-04	4.30E-02
UP_KEYWORDS	Chromosome	18	2.10E-04	6.80E-03
GOTERM_CC_DIRECT	kinetochore	7	2.30E-03	1.90E-01
GOTERM_BP_DIRECT	chromosome segregation	4	1.10E-01	1.00E+00
Annotation Cluster 2: Enrichment Score: 2.61				
GOTERM_BP_DIRECT	mRNA splicing, via spliceosome	14	1.30E-04	4.20E-02
UP_KEYWORDS	mRNA processing	16	2.50E-04	7.60E-03
KEGG_PATHWAY	Spliceosome	10	7.60E-04	1.50E-01
GOTERM_CC_DIRECT	catalytic step 2 spliceosome	8	8.60E-04	9.90E-02
UP_KEYWORDS	mRNA splicing	13	8.60E-04	2.40E-02
UP_KEYWORDS	Spliceosome	8	3.90E-03	9.50E-02
GOTERM_MF_DIRECT	RNA binding	19	7.20E-03	6.90E-01
GOTERM_BP_DIRECT	RNA splicing	7	6.80E-02	1.00E+00
GOTERM_BP_DIRECT	mRNA processing	7	9.10E-02	1.00E+00
Annotation Cluster 3: Enrichment Score: 1.88				
GOTERM_CC_DIRECT	catalytic step 2 spliceosome	8	8.60E-04	9.90E-02
UP_KEYWORDS	Spliceosome	8	3.90E-03	9.50E-02
SMART	Sm	3	4.10E-02	9.50E-01
INTERPRO	Ribonucleoprotein LSM domain	3	4.70E-02	9.70E-01
INTERPRO	Like-Sm (LSM) domain	3	6.00E-02	9.80E-01
Annotation Cluster 4: Enrichment Score: 1.82				
GOTERM_BP_DIRECT	RNA processing	7	6.70E-03	7.00E-01
UP_KEYWORDS	Viral nucleoprotein	4	9.30E-03	1.90E-01
GOTERM_CC_DIRECT	viral nucleocapsid	4	1.10E-02	3.60E-01
UP_KEYWORDS	Ribonucleoprotein	11	1.90E-02	2.80E-01
GOTERM_CC_DIRECT	intracellular ribonucleoprotein complex	7	2.60E-02	5.30E-01
UP_KEYWORDS	Virion	4	3.70E-02	4.10E-01
Annotation Cluster 5: Enrichment Score: 1.63				
SMART	WD40	11	8.30E-03	6.90E-01
UP_SEQ_FEATURE	repeat:WD 3	11	1.20E-02	1.00E+00
UP_KEYWORDS	WD repeat	11	1.40E-02	2.20E-01
INTERPRO	WD40-repeat-containing domain	12	1.40E-02	1.00E+00
UP_SEQ_FEATURE	repeat:WD 6	9	1.40E-02	9.90E-01
UP_SEQ_FEATURE	repeat:WD 5	10	1.40E-02	9.60E-01
INTERPRO	WD40 repeat	11	1.40E-02	9.90E-01
UP_SEQ_FEATURE	repeat:WD 1	11	1.40E-02	9.30E-01

UP_SEQ_FEATURE	repeat:WD 2	11	1.40E-02	9.30E-01
UP_SEQ_FEATURE	repeat:WD 4	10	2.20E-02	9.70E-01
INTERPRO	WD40/YVTN repeat-like-containing domain	12	2.30E-02	9.90E-01
UP_SEQ_FEATURE	repeat:WD 7	5	2.20E-01	1.00E+00
INTERPRO	WD40 repeat, conserved site	4	5.20E-01	1.00E+00
Annotation Cluster 6: Enrichment Score: 1.43				
GOTERM_BP_DIRECT	kynurenine metabolic process	3	1.70E-03	3.30E-01
GOTERM_MF_DIRECT	kynurenine-oxoglutarate transaminase activity	3	1.70E-03	3.50E-01
INTERPRO	Pyridoxal phosphate-dependent transferase, major region, subdomain 2	4	2.50E-02	9.80E-01
INTERPRO	Aminotransferase, class I/classII	3	3.20E-02	9.60E-01
INTERPRO	Pyridoxal phosphate-dependent transferase	4	3.40E-02	9.50E-01
INTERPRO	Pyridoxal phosphate-dependent transferase, major region, subdomain 1	4	3.40E-02	9.50E-01
UP_KEYWORDS	Aminotransferase	3	4.60E-02	4.40E-01
GOTERM_MF_DIRECT	pyridoxal phosphate binding	4	7.60E-02	9.90E-01
UP_KEYWORDS	Pyridoxal phosphate	4	7.60E-02	5.60E-01
GOTERM_BP_DIRECT	biosynthetic process	3	9.40E-02	1.00E+00
KEGG_PATHWAY	Tryptophan metabolism	3	1.70E-01	9.60E-01
GOTERM_MF_DIRECT	catalytic activity	4	6.30E-01	1.00E+00
Annotation Cluster 7: Enrichment Score: 1.07				
UP_KEYWORDS	DNA damage	13	9.80E-03	1.80E-01
UP_KEYWORDS	Fanconi anemia	3	3.50E-02	4.00E-01
KEGG_PATHWAY	Fanconi anemia pathway	4	7.50E-02	9.30E-01
UP_KEYWORDS	DNA repair	7	3.20E-01	8.80E-01
GOTERM_BP_DIRECT	DNA repair	5	5.80E-01	1.00E+00

Table S2. Functional annotation of genes associated with increased longevity in birds. Related to Figure 2. Gene ontology (GO) functional categorization of genes where mean dn/ds values significantly differed between high- and regular-longevity birds (Bonferroni corrected p-value < 0.05). BP: biological process, MF: molecular function.

We identified TERT as a gene under strong selective pressure in HL birds relative to RL birds. While protective against cell senescence, a risk of high TERT activity is an increased rate of uncontrolled proliferation and tumor formation [S11]. Highlighting the importance of balancing these processes, we found genes under selective pressure in long-lived birds were enriched for processes related to cell proliferation and tumor suppression (Annotation Cluster 1). These include: BUB1B and BUB3, both mitotic checkpoint proteins that regulate the spindle assembly machinery during cell division and previously known longevity factors [S12]; KIF4A and KIF1BP, components of a microtubule-based motor protein that regulates cell division, proliferation, and cancer progression by controlling chromosome integrity during mitosis (overlapping in function with BUB genes) [S13]; and CCNE1, a member of the cyclin family implicated in cell cycling, chromosomal stability, and tumorigenesis [S14]. For complete set of genes under differential selection in HL versus RL birds please see Data S1D.

Species	Sequenced Genome Size	Sequencing depth – technology used	Number of scaffolds	N50 scaffold	N50 contig	Reference
Chicken	1.07 Gb	7x – Sanger	16,847	7.07 Mb	36 kb	[S15]
Zebra finch	1.2 Gb	6x – Sanger	37,422	10.4 Mb	39 kb	[S16]
Budgerigar	1.23 Gb	160x – Hybrid	25,212	10.6 Mb	55.6 kb	[S17, S18]
Puerto-Rican Parrot	1.18 Gb	24x – Illumina	148,255	19.2 kb	6.9 kb	[S19]
Scarlet Macaw	0.99 Gb	26x – Hybrid	192,790	16.0 kb	4.4 kb	[S20]
Kea	1.05 Gb	32x – Illumina	42,180	61.4 kb	26.5 kb	[S21]
Peach-faced Lovebird	1.12 Gb	100x – Illumina	52,900	118.3 kb	28.6 kb	[S22]
Blue-fronted Amazon	1.28 Gb	120.6x – Hybrid	3,128	1.09 Mb	27.8 kb	This study

Table S3. Assembly statistics for the Blue-fronted Amazon in the context of the initial releases of other avian genomes. Related to STAR Methods. The size of the *Amazona aestiva* draft genome assembly is similar to those of other high-coverage sequenced avian genomes, with 88% of the estimated genome size assembled with gaps and 82% without gaps. By comparison, the Puerto Rican Parrot, Scarlet Macaw, and Kea assemblies are much more discontinuous (148,255; 192,790; and 42,180 scaffolds, respectively [S19-21]), likely due to lower coverage, library insert sizes, and the longer 454 reads. Although the Illumina plus 454 assembled budgerigar genome has a higher N50 scaffold size statistic (10.6 Mb), that assembly is also split into substantially more scaffolds (25,212) with a larger range of fragment sizes and lower mean sequence length than the Blue-fronted Amazon assembly (44,319 bp and 349,524 bp, respectively) [S18]. *International Chicken Genome Consortium.

Transposable Element Class	RepeatMasker		RepeatModeler		MITE-Hunter		Total		Number of TE units
	bp	%	bp	%	bp	%	bp	%	
Retrotransposons									
SINEs	17,515	0.002%	48,504	0.004%	NA	NA	64,251	0.01%	187
LINEs	68,848,293	6.095%	33,069,485	2.927%	NA	NA	80,618,676	7.14%	122,178
LTR elements	3,142,254	0.278%	6,049,894	0.536%	NA	NA	7,195,515	0.64%	19,039
DNA transposons									
MITEs	3,756	0.000%	2,358	0.000%	23,227,765	2.06%	23,233,879	2.06%	26,317
Other	99,371	0.009%	71,263	0.006%	NA	NA	168,990	0.02%	800
Unclassified	4,203,118	0.372%	26,133,317	2.313%	15,249,652	1.35%	26,881,654	2.38%	99.278
Total	**76,314,307**	**6.755%**	**65,374,821**	**5.787%**	**38,477,417**	**3.41%**	**138,162,965**	**12.23%**	**267.799**

Table S4. Repeat content of the Blue-fronted Amazon genome. Related to STAR Methods. Numbers indicate length of repeats in base pairs (bp), their corresponding percentage of genome (%), and numbers of TE units.

The 12.23% total repetitive sequence content of the Blue-fronted Amazon genome at first appears substantially higher than in most other avian genomes. Previously the chicken and zebra finch repetitive sequences were initially reported at 8.5% [S15] and 7.7% [S16], respectively, and more recently similar figures were reported for other species [S20, S23]. The exception has been the Downy Woodpecker, where LINE content alone accounts for 18% of genomic sequence [S21]. We believe that the high value for the Blue-fronted Amazon genome is potentially due to the application of multiple repeat finding strategies, as seen in other studies [S24]. Indeed, we observed a much higher proportion of repetitive genomic sequence with a combined approach (12.23%) than with RepeatMasker only (6.75%). Supporting this observation, a recent study that also used a combination of repeat-finding methodologies reported higher repetitive sequence content estimates than earlier analyses in chicken (13.28%) and zebra finch (12.83%) [S25], although estimates were still low for other avian species in the same work (Peregrine Falcon, 6.69%; Saker Falcon, 6.80%; turkey, 9.62%). The fact that avian genomes with the highest levels of sequence coverage, including Blue-fronted Amazon, present the highest estimates of repetitive content, suggests that high coverage sequencing may be required for more accurate estimates of repetitive genomic sequence. These values are still all lower than in mammals, where repetitive sequence elements account for a large proportion of the total genome sequence, with estimates of up to 45% in humans [S26].

UCNE ID	Average sequence deviation, parrots	Average sequence deviation, non-parrots	phylogenetic ANOVA	UCNE length (bp)
chr8_Ariane	10%	3%	9.99E-04	208
chr21_Gandalf	10%	3%	9.99E-03	200
ZC3H3_Roxane	7%	1%	9.99E-04	257
AUTS2_Ariel	7%	3%	1.20E-02	214
MIR4307_Noah	7%	4%	2.50E-02	224
ZNF608_Scheherazade	7%	4%	4.10E-02	299
BCL11A_Xavier	6%	1%	9.99E-04	201
chr5_Mateo	6%	2%	2.00E-03	208
SP8_Scarlett	6%	2%	7.99E-03	215
chr17_Bryan	6%	2%	1.50E-02	274
chr3_Eduardo	5%	2%	2.00E-03	294
chr15_Chen	5%	2%	3.00E-03	516
NPAS3_Jacob	5%	2%	4.00E-03	243
PROX1_Pablo	5%	1%	7.99E-03	208
ERBB4_Scheherazade	5%	2%	7.99E-03	247
SOX6_Julia	5%	2%	2.40E-02	250
chr2_Naomi	5%	2%	3.10E-02	206
ESRRG_Isolde	5%	2%	3.80E-02	213
EBF3_Isaac	5%	3%	4.60E-02	276
BCL11A_Zeus	5%	3%	4.95E-02	203

Table S5. Ultra-conserved noncoding elements (UCNEs) divergent in parrots. Related to STAR Methods. Consensus chicken sequences for 4,351 UCNEs were obtained from a previous analysis [S27]. 20 of these were found to be divergent in parrots from the consensus chicken sequence by 5% or more, and significantly more divergent in parrots relative to other avian genomes (phylogenetic ANOVA, $\alpha < 0.05$).

Supplemental References

S1. Tsolou, A., Nelson, G., Trachana, V., Chondrogianni, N., Saretzki, G., von Zglinicki, T., and Gonos, E.S. (2012). The 19S proteasome subunit Rpn7 stabilizes DNA damage foci upon genotoxic insult. IUBMB Life *64*, 432-442.

S2. Filippov, V., Filippova, M., and Duerksen-Hughes, P.J. (2007). The Early Response to DNA Damage Can Lead to Activation of Alternative Splicing Activity Resulting in CD44 Splice Pattern Changes. Cancer Research *67*, 7621-7630.

S3. Lei, K., Zhu, X., Xu, R., Shao, C., Xu, T., Zhuang, Y., and Han, M. (2012). Inner Nuclear Envelope Proteins SUN1 and SUN2 Play a Prominent Role in the DNA Damage Response. Current Biology *22*, 1609-1615.

S4. Elhassan, M.O., Christie, J., and Duxbury, M.S. (2012). Homo sapiens Systemic RNA Interference-defective-1 Transmembrane Family Member 1 (SIDT1) Protein Mediates Contact-dependent Small RNA Transfer and MicroRNA-21-driven Chemoresistance. Journal of Biological Chemistry *287*, 5267-5277.

S5. Xiong, D., Li, G., Li, K., Xu, Q., Pan, Z., Ding, F., Vedell, P., Liu, P., Cui, P., Hua, X., et al. (2012). Exome sequencing identifies MXRA5 as a novel cancer gene frequently mutated in non–small cell lung carcinoma from Chinese patients. Carcinogenesis *33*, 1797-1805.

S6. Prabhakar, S., Noonan, J.P., Pääbo, S., and Rubin, E.M. (2006). Accelerated Evolution of Conserved Noncoding Sequences in Humans. Science *314*, 786-786.

S7. Pollard, K.S., Salama, S.R., King, B., Kern, A.D., Dreszer, T., Katzman, S., Siepel, A., Pedersen, J.S., Bejerano, G., Baertsch, R., et al. (2006). Forces Shaping the Fastest Evolving Regions in the Human Genome. PLoS Genet *2*, e168.

S8. Jarvis, E.D., Mirarab, S., Aberer, A.J., Li, B., Houde, P., Li, C., Ho, S.Y.W., Faircloth, B.C., Nabholz, B., Howard, J.T., et al. (2014). Whole-genome analyses resolve early branches in the tree of life of modern birds. Science *346*, 1320-1331.

S9. Tacutu, R., Craig, T., Budovsky, A., Wuttke, D., Lehmann, G., Taranukha, D., Costa, J., Fraifeld, V.E., and de Magalhães, J.P. (2013). Human Ageing Genomic Resources: Integrated databases and tools for the biology and genetics of ageing. Nucleic Acids Research *41*, D1027-D1033.

S10. Prinzinger, R. (1993). Life span in birds and the ageing theory of absolute metabolic scope. Comparative Biochemistry and Physiology Part A: Physiology *105*, 609-615.

S11. Kim, N.W., Piatyszek, M.A., Prowse, K.R., Harley, C.B., West, M.D., Ho, P.L., Coviello, G.M., Wright, W.E., Weinrich, S.L., and Shay, J.W. (1994). Specific association of human telomerase activity with immortal cells and cancer. Science *266*, 2011-2015.

S12. Elowe, S. (2011). Bub1 and BubR1: at the Interface between Chromosome Attachment and the Spindle Checkpoint. Molecular and Cellular Biology *31*, 3085-3093.

S13. Wu, G., Zhou, L., Khidr, L., Guo, X.E., Kim, W., Lee, Y.M., Krasieva, T., and Chen, P.-L. (2008). A novel role of the chromokinesin Kif4A in DNA damage response. Cell Cycle *7*, 2013-2020.

S14. Loeb, K.R., Kostner, H., Firpo, E., Norwood, T., D. Tsuchiya, K., Clurman, B.E., and Roberts, J.M. (2005). A mouse model for cyclin E-dependent genetic instability and tumorigenesis. Cancer Cell *8*, 35-47.

S15. Hillier, L.W., Miller, W., Ewan Birney , Warren, W., Hardison, R.C., Ponting, C.P., Bork, P., Burt, D.W., Groenen, M.A.M., Delany, M.E., et al. (2004). Sequence and comparative analysis of the chicken genome provide unique perspectives on vertebrate evolution. Nature *432*, 695-716.

S16. Warren, W.C., Clayton, D.F., Ellegren, H., Arnold, A.P., Hillier, L.W., Kunstner, A., Searle, S., White, S., Vilella, A.J., Fairley, S., et al. (2010). The genome of a songbird. Nature *464*, 757-762.

S17. Koren, S., Schatz, M.C., Walenz, B.P., Martin, J., Howard, J.T., Ganapathy, G., Wang, Z., Rasko, D.A., McCombie, W.R., Jarvis, E.D., et al. (2012). Hybrid error correction and *de novo* assembly of single-molecule sequencing reads. Nat Biotech *30*, 693-700.

S18. Ganapathy, G., Howard, J., Ward, J., Li, J., Li, B., Li, Y., Xiong, Y., Zhang, Y., Zhou, S., Schwartz, D., et al. (2014). High-coverage sequencing and annotated assemblies of the budgerigar genome. GigaScience *3*, 11.

S19. Oleksyk, T., Pombert, J.-F., Siu, D., Mazo-Vargas, A., Ramos, B., Guiblet, W., Afanador, Y., Ruiz-Rodriguez, C., Nickerson, M., Logue, D., et al. (2012). A locally funded Puerto Rican parrot (*Amazona vittata*) genome sequencing project increases avian data and advances young researcher education. GigaScience *1*, 14.

S20. Seabury, C.M., Dowd, S.E., Seabury, P.M., Raudsepp, T., Brightsmith, D.J., Liboriussen, P., Halley, Y., Fisher, C.A., Owens, E., Viswanathan, G., et al. (2013). A Multi-Platform Draft *de novo* Genome Assembly and Comparative Analysis for the Scarlet Macaw (*Ara macao*). PLoS ONE *8*, e62415.

S21. Zhang, G., Li, C., Li, Q., Li, B., Larkin, D.M., Lee, C., Storz, J.F., Antunes, A., Greenwold, M.J., Meredith, R.W., et al. (2014). Comparative genomics reveals insights into avian genome evolution and adaptation. Science *346*, 1311-1320.

S22. van der Zwan, H., van der Westhuizen, F., Visser, C., and van der Sluis, R. (2017). Draft De Novo Genome Sequence of Agapornis roseicollis for Application in Avian Breeding. Animal Biotechnology, 1-6.

S23. Doyle, J.M., Katzner, T.E., Bloom, P.H., Ji, Y., Wijayawardena, B.K., and DeWoody, J.A. (2014). The Genome Sequence of a Widespread Apex Predator, the Golden Eagle (*Aquila chrysaetos*). PLoS ONE *9*, e95599.

S24. Lerat, E. (2010). Identifying repeats and transposable elements in sequenced genomes: how to find your way through the dense forest of programs. Heredity *104*, 520-533.

S25. Zhan, X., Pan, S., Wang, J., Dixon, A., He, J., Muller, M.G., Ni, P., Hu, L., Liu, Y., Hou, H., et al. (2013). Peregrine and saker falcon genome sequences provide insights into evolution of a predatory lifestyle. Nat Genet *45*, 563-566.

S26. International Human Genome Sequencing Consortium (2001). Initial sequencing and analysis of the human genome. Nature *409*, 860-921.

S27. Dimitrieva, S., and Bucher, P. (2013). UCNEbase—a database of ultraconserved non-coding elements and genomic regulatory blocks. Nucleic Acids Research *41*, D101-D109.